Electronic Supplementary Information

Intrinsic white-light-emitting hyperbranched polyimide: synthesis, structure-property and its application as "turn-off" sensor for iron(III) ions

An Xing[1,2], Xuepei Miao[1,†], Tuan Liu[1,‡], Haoran Yang[1], Yan Meng[1,*], Xiaoyu Li[2,*]

[1]Key Laboratory of Carbon Fiber and Functional Polymers, Ministry of Education, Beijing University of Chemical Technology, Beijing 100029, P. R. China

[2]State Key Laboratory of Organic-Inorganic Composites, Beijing University of Chemical Technology, Beijing 100029, P. R. China

Correspondence to: Y. Meng (Email: mengyan@mail.buct.edu.cn; Fax: +86-10-64452129; Tel: +86-10-64419631); X. Li (E-mail: lixy@mail.buct.edu.cn; Tel: +86-10-64423162).

† Current address: ~~Changzhou Institute of Technology~~

‡ Current address: School of Mechanical and Materials Engineering, Composite Materials and Engineering Center, Washington State University, Pullman, Washington 99164, USA

Table of Contents Page number

Synthesis of linear semialiphatic polyimides (LBPA)

2.28 g (10 mmol) bisphenol A, 35 mL toluene and 30 mL dimethylsulfoxide were charged into a 100 mL three-necked flask, which was equipped with a magnetic stirrer, a thermometer, a Dean-Stark trap, a condenser, and a nitrogen inlet. After removal of air by bubbling nitrogen, 1.38 g (10 mmol) K_2CO_3 were added into the flask under stirring. The temperature was then raised and held at 175 ^oC until complete removal of toluene/water azeotrope. The azeotrope started to remove at 145 ^oC. After cooling to room temperature, 4.77 g (10 mmol) A_2-3 were added. The temperature was increased and kept at 150 ^oC for 10 hours. After cooling, the mixtures were slowly poured into 120 mL methanol to precipitate products. The crude products were collected, reprecipitated from THF to ethanol/water (volume ratio 1:1) mixture twice. Finally, it was dried in vacuum at 90 ^oC. Yield: 58%. IR (KBr): 1772, 1712, 1600, 1389, 1271, 1232, 745 cm^{-1}. ^1H NMR (400 MHz, (methylsulphoxide)-d_6, δ): 1.65 (t, CH_3-), 3.43 (s, OCH_2-), 3.51 (s, OCH_2-), 3.62 (s, NCH_2-), 6.67-7.78 (br, C_6H_4O or C_6H_3O). M_n=6880 $g.mol^{-1}$, PDI=1.79.

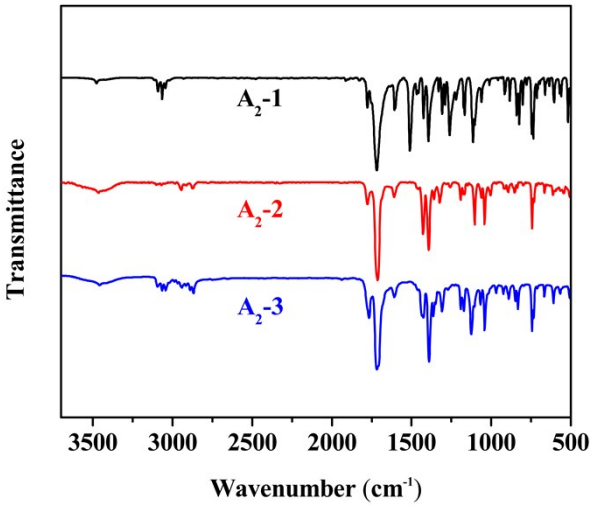

Figure S1. FTIR spectra of A_2 monomers (A_2-1, A_2-2, A_2-3, from top to bottom).

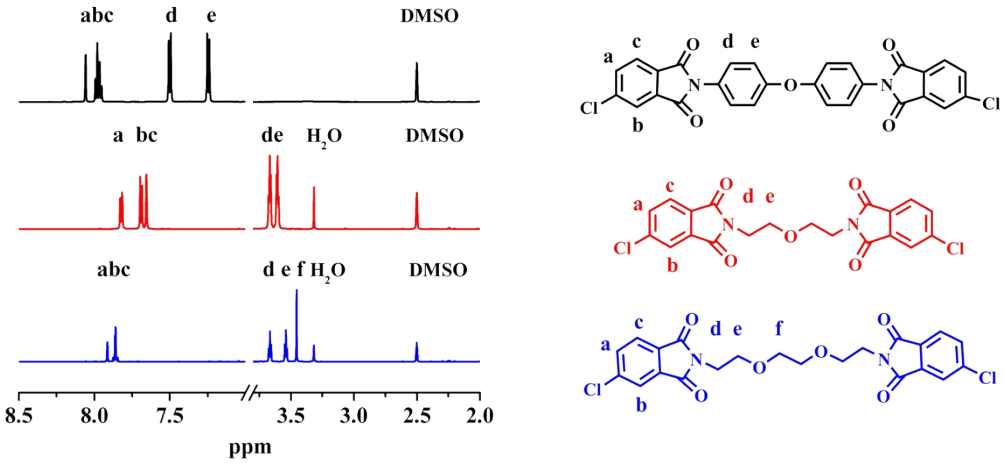

Figure S2. ^{1}H NMR spectra of A_2 monomers (A_2-1, A_2-2, A_2-3, from top to bottom).

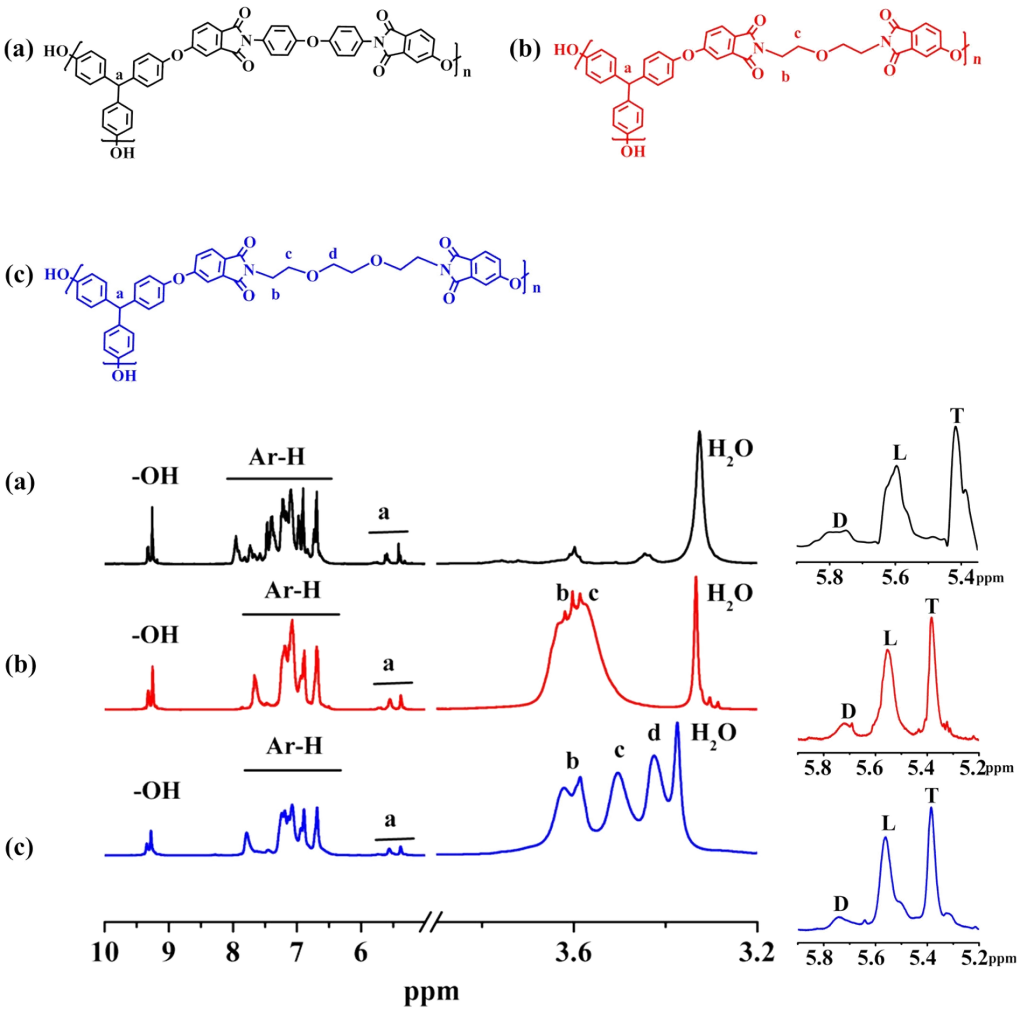

Figure S3. ^{1}H NMR spectra and assignments of the dendritic, terminal and linear units of (a) HBPI1, (b) HBPI2, and (c) HBPI3.

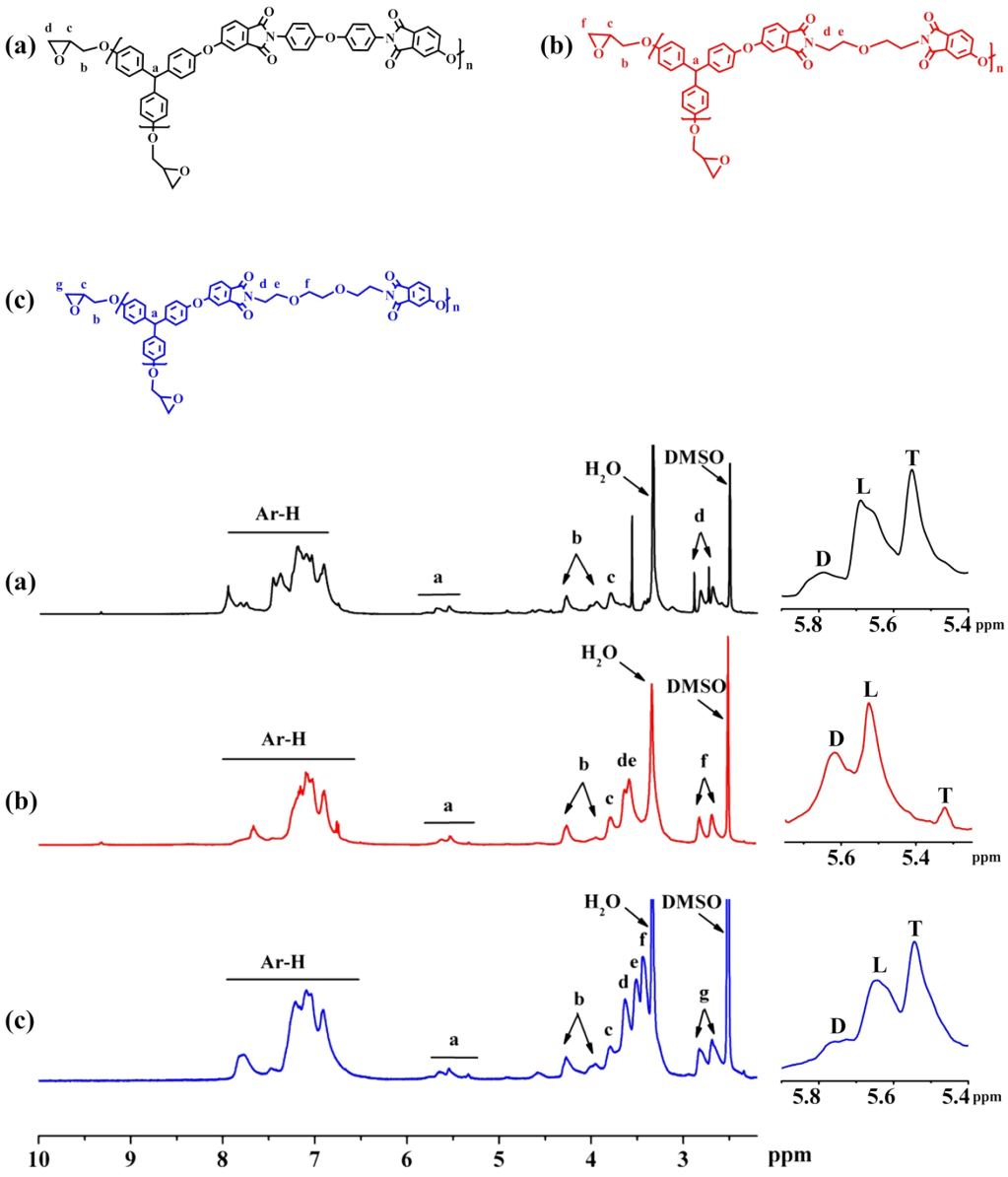

Figure S4. ^{1}H NMR spectra and assignments of the dendritic, terminal and linear units of (a) EHBPI1, (b) EHBPI2, and (c) EHBPI3.

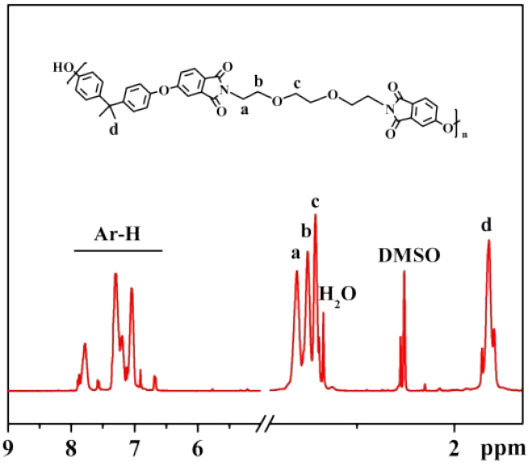

Figure S5. ^{1}H NMR spectra of LBPA.

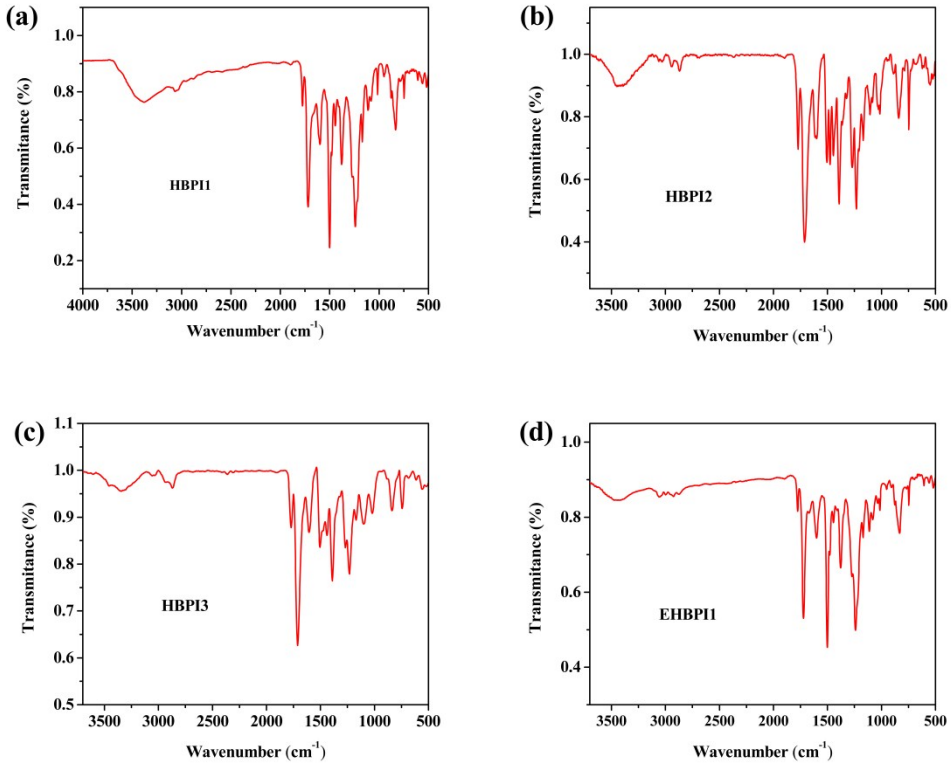

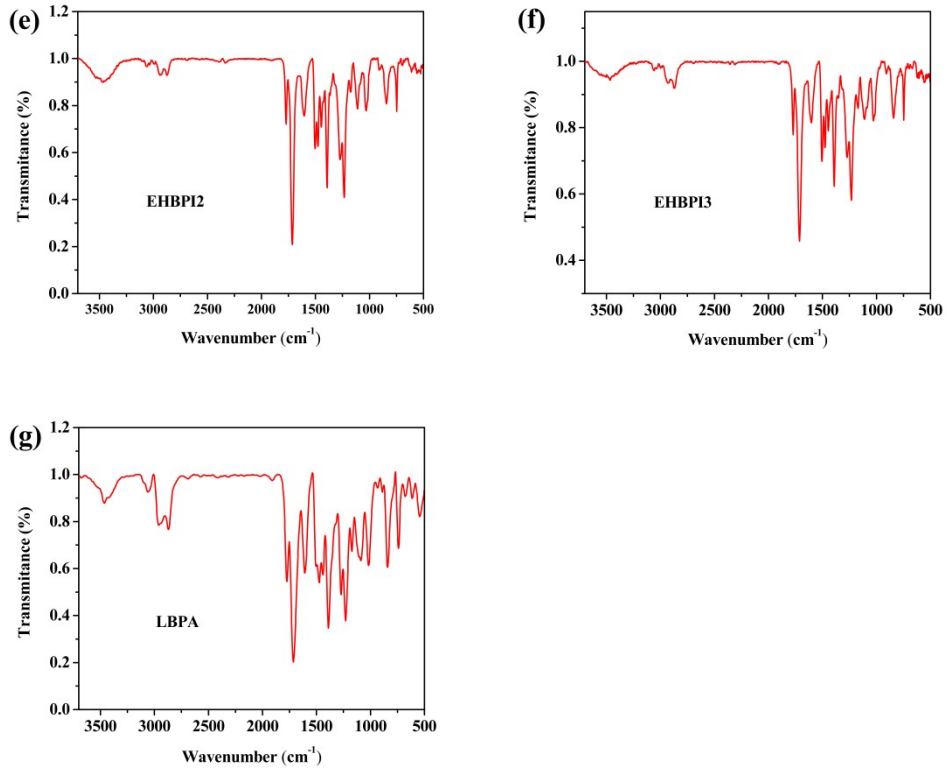

Figure S6. FTIR spectra of (a) HBPI1, (b) HBPI2, (c) HBPI3, (d) EHBPI1, (e) EHBPI2, (f) EHBPI3, and (g) LBPA.

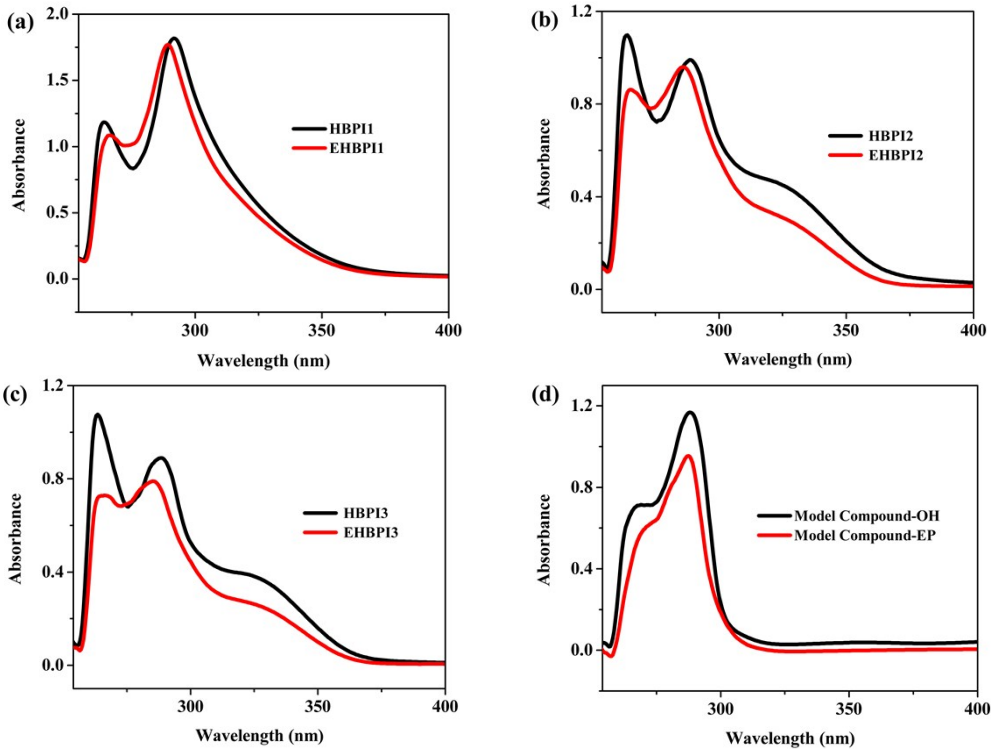

Figure S7. UV/Vis absorption spectra of solutions of (a) HBPI1 and EHBPI1, (b) HBPI2 and EHBPI2, (c) HBPI3 and EHBPI3, (d) model compound-OH and model

compound-EP (The structures of model compound-OH and model compound-EP are shown in Scheme S1).

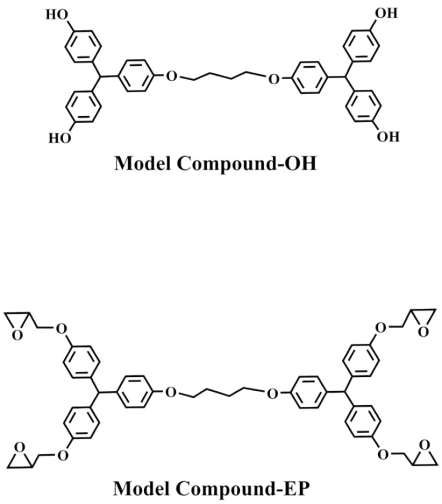

Scheme S1. Structures of model compound-OH and model compound-EP.

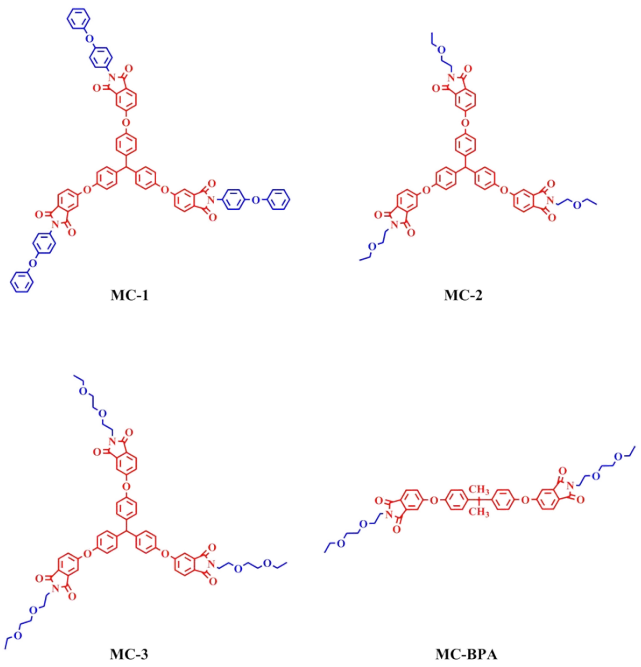

Scheme S2. Structures of model compounds for TD-DFT calculations.

MC-1	MC-2	MC-3	MC-3-solid	MC-BPA
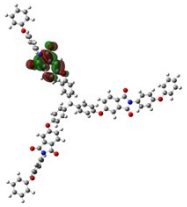	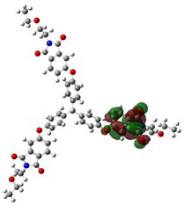	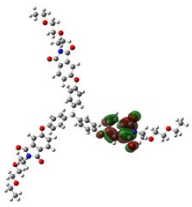	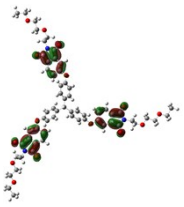	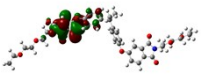
LUMO+2	LUMO+2	LUMO+2	LUMO+2	LUMO+2
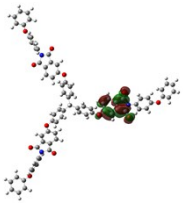	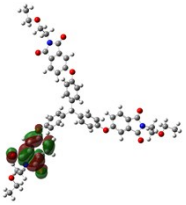	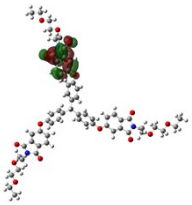		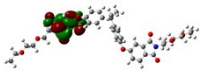
LUMO+1	LUMO+1	LUMO+1	LUMO+1	LUMO+1
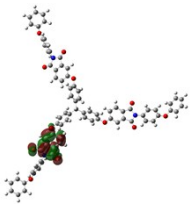	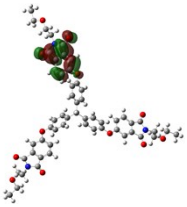	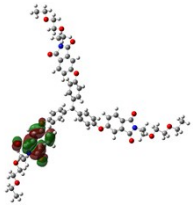	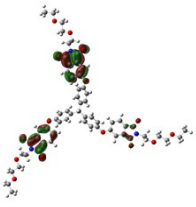	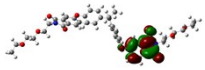
LUMO	LUMO	LUMO	LUMO	LUMO
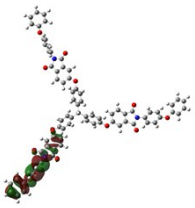	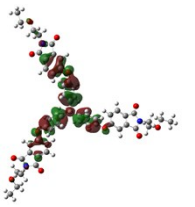	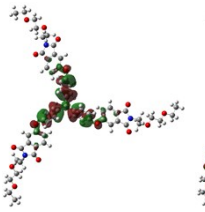		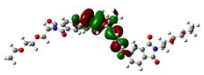
HOMO	HOMO	HOMO	HOMO	HOMO
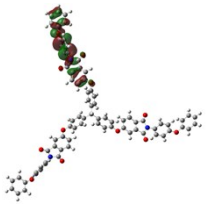	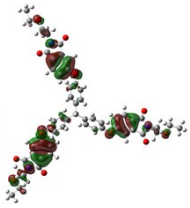	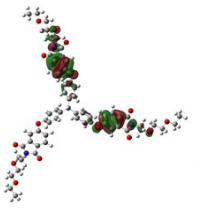		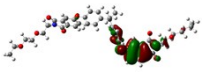
HOMO-1	HOMO-1	HOMO-1	HOMO-1	HOMO-1
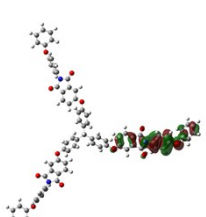	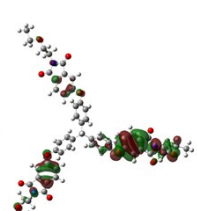	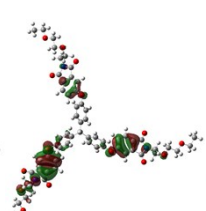	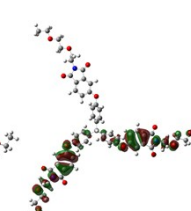	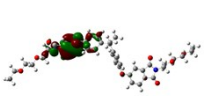
HOMO-2	HOMO-2	HOMO-2	HOMO-2	HOMO-2

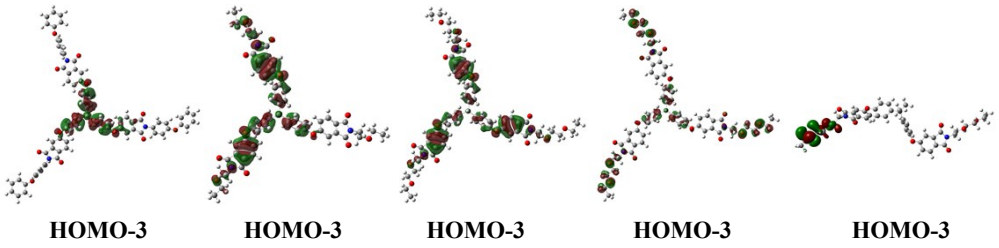

Figure S8. Calculated molecular orbitals of MC-1, MC-2, MC-3 and MC-BPA (TD-DFT method at the B3LYP/6-311++G(d,p) scrf=(solvent=~~N,N-dimethyl- formamide~~) level), MC-3-solid (TD-DFT method at the B3LYP/6-311++G(d,p) level). HOMO-m and LUMO+m denote the (m+1)th highest occupied orbital and the (m+1)th lowest unoccupied orbital, respectively.

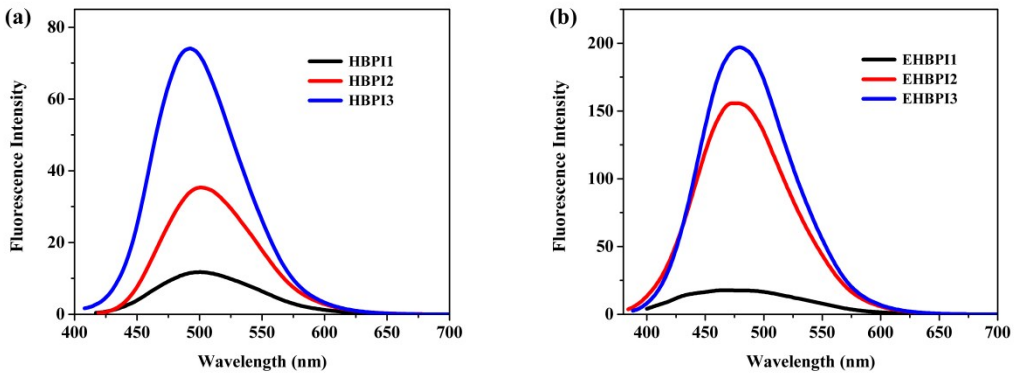

Figure S9. Fluorescence spectra of solutions of (a) HBPIs, and (b) EHBPIs excited at their optimal excitation wavelength respectively.

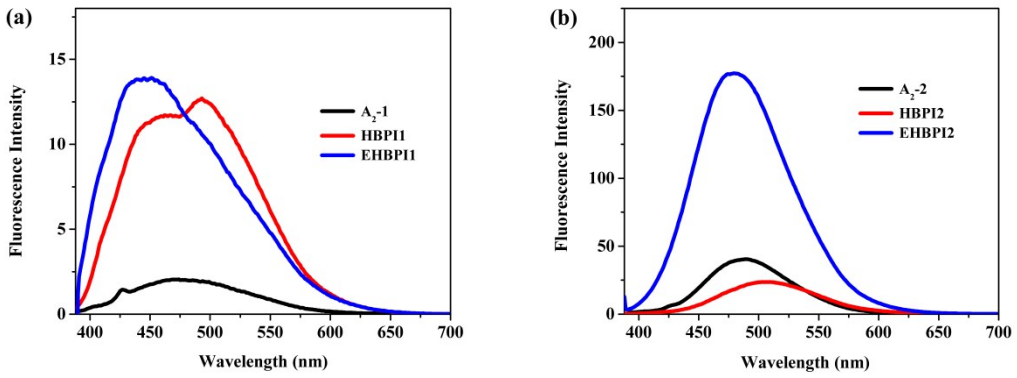

Figure S10. Fluorescence spectra of solutions of (a) A_2-1 and polyimides derived from A_2-1, (b) A_2-2 and polyimides derived from A_2-2.

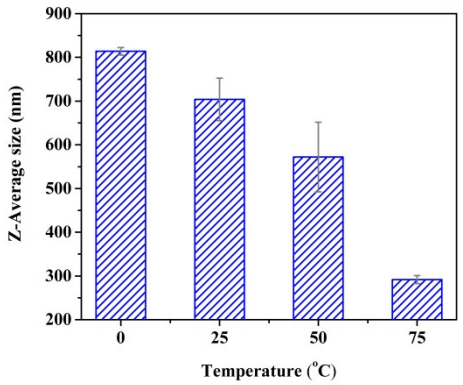

Figure S11. The effects of temperature on the particle diameters of EHBPI3 aggregates in EHBPI3/NMP/H_2O (37.5%) system. The z-average sizes of aggregates were measured by Malvern Zeta-sizer Nano-ZS at different temperatures (15, 25, 50 and 70 °C) and particle size data was averaged over 3 runs.

Table S1. Transition wavelengths, oscillator strengths, orbitals, assignments of $S_0 \rightarrow S_i$ transition, and contributions of each transition of model compounds.

System	State	Transition Wavelength/nm	Oscillator Strength	Orbitals	Assignment of Transition	Contribution
MC-1	1	386.7	0.0020	HOMO → LUMO	CT	0.94
	2	383.1	0.0028	HOMO-1 → LUMO+2	CT	0.95
	3	382.3	0.0030	HOMO-2 → LUMO+1	CT	0.95
MC-2	1	344.3	0.0525	HOMO → LUMO	HLCT	0.28
				HOMO-1 → LUMO	HLCT	0.27
				HOMO-3 → LUMO	HLCT	0.32
	2	343.4	0.0459	HOMO → LUMO+1	HLCT	0.16
				HOMO-1 → LUMO+1	HLCT	0.39
				HOMO-2 → LUMO+1	HLCT	0.12
				HOMO-3 → LUMO+1	HLCT	0.26
	3	342.4	0.0427	HOMO-1 → LUMO+2	HLCT	0.20
				HOMO-2 → LUMO+2	HLCT	0.74
MC-3	1	341.8	0.0587	HOMO → LUMO	CT	0.03
				HOMO → LUMO+1	CT	0.02
				HOMO-1 → LUMO+1	HLCT	0.12
				HOMO-2 → LUMO	HLCT	0.29
				HOMO-2 → LUMO+1	HLCT	0.17
				HOMO-3 → LUMO	HLCT	0.17
				HOMO-3 → LUMO+1	HLCT	0.11
	2	341.8	0.0583	HOMO → LUMO+2	CT	0.03
				HOMO-1 → LUMO+1	HLCT	0.06
				HOMO-1 → LUMO+2	HLCT	0.36
				HOMO-2 → LUMO	HLCT	0.09
				HOMO-2 → LUMO+1	HLCT	0.08
				HOMO-2 → LUMO+2	HLCT	0.02
				HOMO-3 → LUMO	HLCT	0.04
				HOMO-3 → LUMO+1	HLCT	0.08
				HOMO-3 → LUMO+2	HLCT	0.14
	3	341.6	0.0312	HOMO → LUMO+2	CT	0.02
				HOMO-1 → LUMO+1	HLCT	0.10
				HOMO-1 → LUMO+2	HLCT	0.24
				HOMO-2 → LUMO	HLCT	0.17
				HOMO-2 → LUMO+1	HLCT	0.09
				HOMO-3 → LUMO	HLCT	0.07
				HOMO-3 → LUMO+1	HLCT	0.08
				HOMO-3 → LUMO+2	HLCT	0.11

System	State	Transition Wavelength/nm	Oscillator Strength	Orbitals	Assignment of Transition	Contribution
MC-3-solid	1	334.0	0.0587	HOMO → LUMO	HLCT	0.35
				HOMO-1 → LUMO	HLCT	0.10
				HOMO-1 → LUMO+1	HLCT	0.05
				HOMO-1 → LUMO+2	HLCT	0.25
				HOMO-2 → LUMO	HLCT	0.04
				HOMO-2 → LUMO+1	HLCT	0.09
				HOMO-3 → LUMO	CT	0.02
	2	333.9	0.0586	HOMO → LUMO+1	HLCT	0.35
				HOMO-1 → LUMO	HLCT	0.05
				HOMO-1 → LUMO+1	HLCT	0.09
				HOMO-2 → LUMO	HLCT	0.10
				HOMO-2 → LUMO+1	HLCT	0.04
				HOMO-2 → LUMO+2	HLCT	0.26
				HOMO-3 → LUMO+1	CT	0.02
	3	333.4	0.0064	HOMO → LUMO+2	HLCT	0.35
				HOMO-1 → LUMO	HLCT	0.23
				HOMO-1 → LUMO+1	HLCT	0.04
				HOMO-2 → LUMO	HLCT	0.04
				HOMO-2 → LUMO+1	HLCT	0.25
				HOMO-3 → LUMO+2	CT	0.02
MC-BPA	1	342.7	0.0858	HOMO-1 → LUMO	HLCT	0.90
	2	337.3	0.0630	HOMO → LUMO+1	HLCT	0.02
				HOMO-2 → LUMO+1	HLCT	0.89
	3	333.3	0.0007	HOMO → LUMO	CT	0.92

Table S2. Optimal excitation wavelengths of HBPIs and EHBPIs.

Hyperbranched Polymers	HBPI1	HBPI2	HBPI3	EHBPI1	EHBPI2	EHBPI3
Optimal Excitation Wavelength (nm)	407	409	396	390	374	378